



Geochronological and Geochemical Constraints on the Petrogenesis of Permian Dolerite Dyke Swarms in the Beishan Orogenic Belt, NW China

Gang Xu¹, Jun Duan^{1*}, Wenbin Gao¹, Rongmin Wang², Zhen Shi¹, Bocheng Ma¹ and Jia Sun³

¹ College of Earth Sciences and Resources, Chang'an University, Xi'an, China, ² Oilfield Development Division of Petrochina Changqing Oilfield Company, Xi'an, China, ³ Tianjin North China Geological Exploration Bureau, Tianjin, China

OPEN ACCESS

Edited by:

Xiaohua Deng,
Beijing Institute of Geology for Mineral
Resources, China

Reviewed by:

Wei Zhang,
China University of Geosciences
Wuhan, China
Joyashish Thakurta,
Western Michigan University,
United States

*Correspondence:

Jun Duan
Duanjun108@163.com

Specialty section:

This article was submitted to
Economic Geology,
a section of the journal
Frontiers in Earth Science

Received: 23 January 2021

Accepted: 26 February 2021

Published: 24 March 2021

Citation:

Xu G, Duan J, Gao W, Wang R,
Shi Z, Ma B and Sun J (2021)
Geochronological and Geochemical
Constraints on the Petrogenesis
of Permian Dolerite Dyke Swarms
in the Beishan Orogenic Belt, NW
China. *Front. Earth Sci.* 9:657716.
doi: 10.3389/feart.2021.657716

Extensive Early Permian mafic-ultramafic intrusions, doleritic dykes, and basalts crop out within the Beishan area, southern Central Asian Orogenic Belt (CAOB). We present new geochronological and geochemical data for Gubaoquan dolerite dyke swarms in the Beishan orogenic belt. Zircon U-Pb Dating of the Gubaoquan dykes indicates that they were emplaced during the Early Permian (280.7 ± 4 Ma), that was coeval with Yinaoxia and Podong mafic dykes in Beishan area. The dykes are characterized by low Mg# (47–84) in the clinopyroxene crystals, and the content of whole-rock Fe_2O_3 (t), MgO, and alkali ($\text{Na}_2\text{O} + \text{K}_2\text{O}$) range from 12.5–17.4, 4.06–5.51, and 2.8–4.4 wt.%, respectively. The samples from the Gubaoquan dykes have high and variable Ba/La (5.93–14.2) and Ba/Nb (15.0–37.3) ratios but low Th/Yb (0.17–0.24) ratios. The rocks show slightly enrichments in LREE, HFSE, Th, and Hf, and depletion in Nb and Ta. The $\epsilon_{\text{Nd}}(t = 280 \text{ Ma})$ values and initial $^{87}\text{Sr}/^{86}\text{Sr}$ ratios of the Gubaoquan dykes show variations ranging from 6.4 to 6.8 and 0.706240 to 0.707546, respectively. These data suggest that the parental magmas for the Gubaoquan dykes were probably derived from partially decompressed melting of upwelling depleted asthenosphere mantle that was metasomatized previously by subducted fluids.

Keywords: Zircon U-Pb dating, Sr-Nd isotopes, Early Permian dolerite dyke swarms, Beishan, Central Asian Orogenic Belt

INTRODUCTION

The Central Asian Orogenic Belt (CAOB) is the important Phanerozoic accretionary orogenic belt in the world (Figure 1A; Sengör et al., 1993; Jahn et al., 2000). It was formed by the amalgamation of accretionary complexes, magmatic arcs, arc-related basins, ophiolites, seamounts, and microcontinents during the long-lived subduction of the Paleo-Asian Ocean (Kröner et al., 2007; Windley et al., 2007; Xiao et al., 2008, 2011, 2019). The Beishan Orogenic Belt is located in the southern margin of the CAOB, and experienced a complex process of tectono-magmatic evolution during the Paleozoic. Therefore, it has become a key part to study the geological evolutionary history of the CAOB. The Early Permian was a crucial period in the evolutionary history of the CAOB, marked by the closure of the Paleo-Asian Ocean, the transition from subduction-accretion to post-collisional tectonism and the occurrence of extensive mantle-derived magmatism

(Wartes et al., 2002; Charvet et al., 2007). The Early Permian (290–270 Ma) magmatism and associated mineralization have been considered as the post-subduction byproducts after the closure of the Paleo-Asian Ocean (Han et al., 2010; Yuan et al., 2010; Song et al., 2011, 2013; Zhang et al., 2011). The petrogenesis of the Early Permian mafic-ultramafic complexes, doleritic dykes, and basalts in the Beishan orogenic belt, and is still in controversial. Zhou et al. (2004) believe that the Permian magmatic rocks in the Tarim area and the adjacent Beishan area together constitute a Large Igneous Province (LIP), which is a product of mantle plume activities (Zhou et al., 2004; Qin et al., 2011; Su et al., 2011, 2012). Zhang et al. (2011) suggest that the Permian mantle-derived coeval in the Beishan area are both products of the post-subduction extension (Zhang et al., 2011; Li et al., 2013, 2020; Zheng et al., 2014). Ao et al. (2010) believe that Permian mafic-ultramafic complexes, such as Pobei and Hongshishan, were formed by subduction process of the Paleo-Asian Ocean, representing the Late Paleozoic island arc settings in the Beishan area (Ao et al., 2010).

Previous studies have mostly focused on the investigation of the Early Permian mafic-ultramafic complex and basalt in the Beishan area, but the petrogenesis of the doleritic dykes is poorly constrained and lack of comparison between different regions, due to the limited geochemical investigations of mafic dykes in this area. As a specific product of tectono-magmatism (Hoek and Seitz, 1995), dolerite dyke swarms can be formed in the marginal areas of the mantle plume-related LIP, the back-arc extension environment and the post-subduction extension settings. The doleritic dykes are important signs of tectono-magmatic evolutionary events and can maximally retain information of mantle source (Halls, 1982; Liu et al., 2013). Thus, they are widely used in reconstructing the aggregation, extension, and breakup of ancient plates (Zhou et al., 2000). In addition, mafic dykes can serve as magma conduits, allowing the transportation of mafic magma from the mantle to the crust and potentially preserving primitive magma compositions that provide crucial information on the nature of the underlying mantle (Adams et al., 2005). Accordingly, we present new geochronological and geochemical data for Gubaoquan mafic dyke swarms in the Beishan area (Figure 1B), and investigate their petrogenesis and the dynamic background. This study aims to provide a basis for further understanding the geotectonic background in Beishan area during Early Permian.

GEOLOGICAL BACKGROUND AND SAMPLE DESCRIPTIONS

Geological Background

The Beishan orogenic belt is located in the southernmost margin of CAOB, adjacent to the Central Tianshan orogenic belt in the north, and the Tarim-North China Craton in the south (Figure 1B). The boundary between CAOB and the North China Craton is the South Tianshan–Liuyuan–Solonker suture zone (Figure 1A), which is considered to represent the final suture zone on the southern margin of CAOB. High-pressure to ultrahigh-pressure metamorphic rock belts related to the

subduction of the Paleo-Asian Ocean are distributed across the suture zone, including Akeyazi blueschist and eclogite in the southwestern Tianshan (Ar–Ar age: 315–319 Ma) (Gao and Klemd, 2003; Klemd, 2003; Klemd et al., 2015; Li et al., 2015), Gubaoquan eclogite in the south of Liuyuan (age of peak metamorphism: ~465 Ma; Liu et al., 2012; Saktura et al., 2017), and the Wenduermiao metamorphic rocks of blueschist facies in Solonker (Ar–Ar age: ~450 Ma) (Gao et al., 1990).

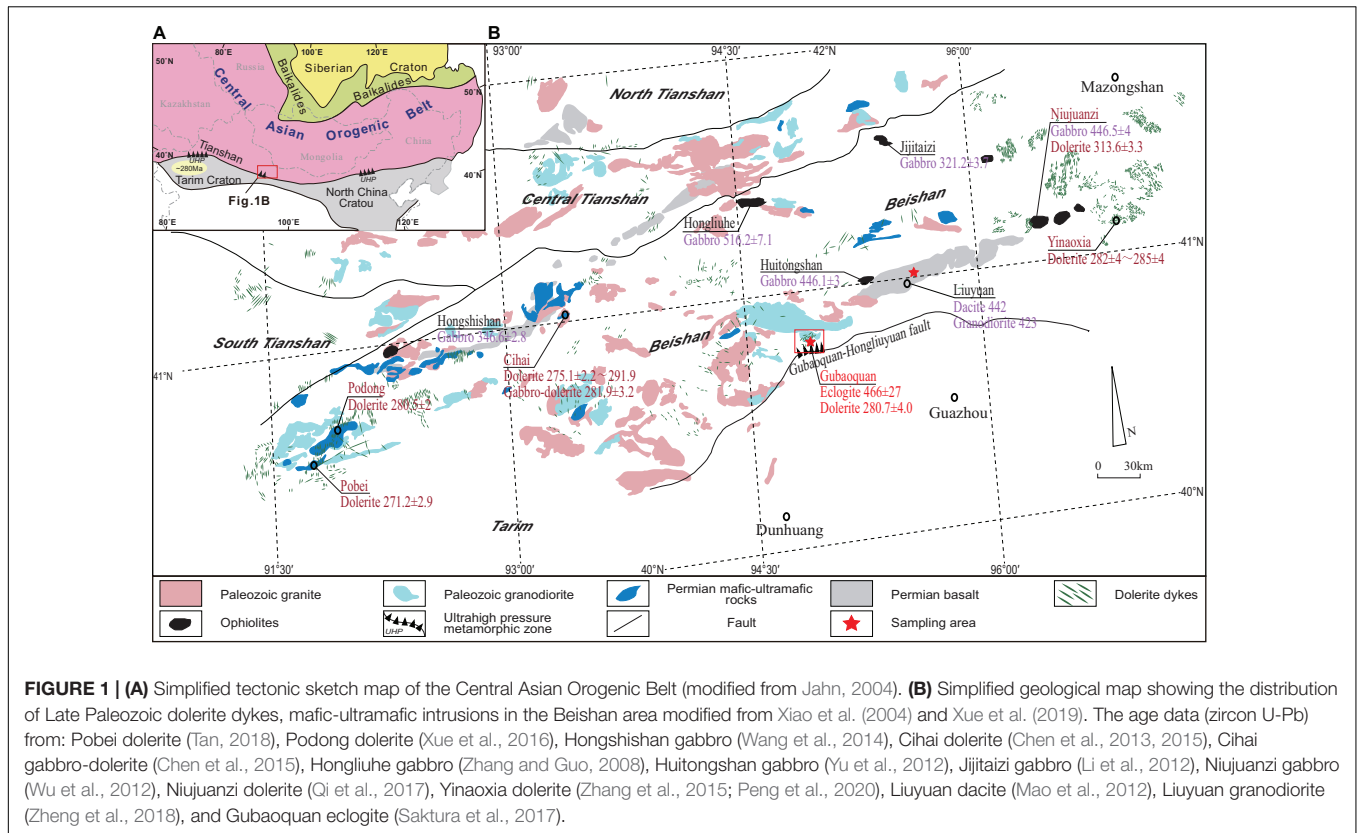
The Beishan orogenic belt evolved from the suturing of several island arcs located in different parts of the Paleo-Asian Ocean during the Early–Middle Paleozoic. The boundaries between the island arcs are the ophiolite belts representing the former oceanic crusts, which are Hongshishan (346.6 ± 2.8 Ma) – Baiheshan–Pengboshan ophiolitic mélange zone (Wang et al., 2014), Jijitaizi (321.2 ± 3.7 Ma) – Xiaohuangshan (336 ± 4 Ma) ophiolitic mélange zone (Li et al., 2012; Zheng et al., 2013), Hongliuhe (516.2 ± 7.1 Ma) – Niujuanzi (446.5 ± 4 Ma) – Xichangjing (536 ± 7 Ma) ophiolitic mélange zone (Zhang and Guo, 2008), and Huitongshan (446.1 ± 3 Ma) – Zhangfangshan (362.6 ± 4 Ma) ophiolitic mélange zone (Yu et al., 2012) from north to south, respectively. In the Beishan area, there are outcrops of Proterozoic to Cenozoic strata, among which, the Precambrian, Ordovician, Silurian, Carboniferous and Permian strata are relatively developed.

Available zircon U–Pb chronological data has shown that there were at least two phases of mafic-ultramafic magmatism in the Beishan area: one from the Late Ordovician to Devonian (360–450 Ma) and the other from the Late Carboniferous to Early Permian (260–305 Ma). The widely distributed ophiolite belts formed during the first stage in the Beishan area includes high-Mg diorite, Nb-rich basalt, normal-mid-oceanic ridge basalt (N-MORB), enriched-MORB (E-MORB), and island arc tholeiite, indicating that the Beishan area may have experienced oceanic crust subduction from the Late Ordovician to Early Devonian (Mao et al., 2012; Zheng et al., 2018). In the later phase, mafic-ultramafic magmatism was frequent, and several mafic-ultramafic complexes and dolerite dyke swarms were developed. These dolerite dykes are extensively distributed across the entire Beishan area and were once associated with the Tarim mantle plume (Xiao et al., 2006).

Permian Mafic Dyke Swarm

The dolerite dyke swarms in the Beishan area are concentrated in the Pobei area in the west, Gubaoquan area in the middle, and Yinwaxia area in the east. Moreover, there are scattered outcrops in other regions (Figure 1B). The dykes are generally parallel, striking toward NW ($310\text{--}355^\circ$) and NE ($10\text{--}80^\circ$), and are nearly vertical (dips of $80^\circ\text{--}90^\circ$; Figure 2E). The dyke swarms predominantly intrude the Silurian–Devonian (380–442 Ma) granodiorite and quartz diorite, as well as the Precambrian to Permian strata (Figures 2A,C,E; Mao, 2008; Mao et al., 2010) in the Liuyuan area. The contact boundaries between the dykes and country rocks and strata are conspicuous (Figures 2A,C,E). Baked edges can be seen between individual dykes and the granodiorite.

The Gubaoquan area is located in the middle section of the southern margin of Beishan in Gansu, to the north of the



Gubaoquan–Hongliuyuan Fault. These dykes generally strike between NNE-NE and NW-SE, and are various in size, with widths ranging from 0.5 to 6 m. Dykes extend from hundreds of meters to thousands of meters, and are nearly vertical (Figure 2E). The Gubaoquan doleritic dykes mainly intrude the Ordovician-Devonian granodiorite, and some of them intrude the metamorphic strata of the Early Paleozoic Huaniushan Group (Figure 1B). The dykes are interspersed in the rock mass and cut through the strata, mostly in apophyses or stocks. The doleritic dykes exposed in the strata generally occur parallel to each other, with greenish-black to dark gray color, and have undergone weak chlorite and sericite alteration (Figure 2F). The dolerite dykes in the granodiorite rock mass are well preserved, mostly in dark green color, and the boundary between the dyke and country rocks is clear and flat (Figure 2E). These mafic dykes contain clinopyroxene (~ 15 vol.%) and plagioclase (~ 10 vol.%) phenocrysts (Figures 2B,D). Matrix minerals are composed of clinopyroxene and plagioclase with minor hornblende and Fe-Ti oxides (Figure 2D). The Gubaoquan doleritic dykes are porphyritic and fresh, with the ophitic textures (Figures 2B,D,F) and comprise the low proportion of Fe-Ti oxides (2 vol.% ~3 vol.%).

ANALYTICAL METHODS

Zircon crystals were separated from a fresh doleritic dyke sample (~25 kg, GBQ-04, 41°00′43.09″N, 95°00′21.52″E) using the

conventional heavy liquid and magnetic separation techniques in a commercial laboratory at Langfang, Hebei Province, China. Representative zircon crystals those were euhedral, colorless, transparent and underformed were mounted in an epoxy resin disk and then polished to analysis. Cathodoluminescence (CL) and back-scattered electron (BSE) images were obtained at the Beijing SHRIMP Center, Institute of Geology, Chinese Academy of Geological Sciences. CL and BSE images were used together to help select the zircon grains that have oscillatory or simple zoning patterns indicative of magmatic crystallization for U-Pb dating.

Zircon U–Pb dating for mafic dykes from the Gubaoquan areas was carried out using LA-ICP-MS at the Key Laboratory of Western China’s Mineral Resources and Geological Engineering, Ministry of Education. Detailed descriptions of the instrumentation and analytical procedures can be found in Luan et al. (2019). A Plešovice zircon (²⁰⁶Pb/²³⁸U age = 337 Ma, Sláma et al., 2008) and Qinghu zircon (²⁰⁶Pb/²³⁸U age = 159 Ma, Li et al., 2009) standard were used as external standard for correcting mass discrimination and isotope fractionation, and Zircon 91500 (²⁰⁷Pb/²⁰⁶Pb age = 1065 Ma, Wiedenbeck, 1995) was analyzed alternately with unknown zircons. Concordia diagrams and weighted mean calculations were carried out using the Isoplot 3.0 program (Ludwig, 2003). Common Pb correction was made using the measured ²⁰⁴Pb and the values of Stacey and Kramers (1975).

Major element concentrations for clinopyroxene and plagioclase were determined by a JEOL JXA-8100 electron microprobe at Chang’an University, China. The analytical

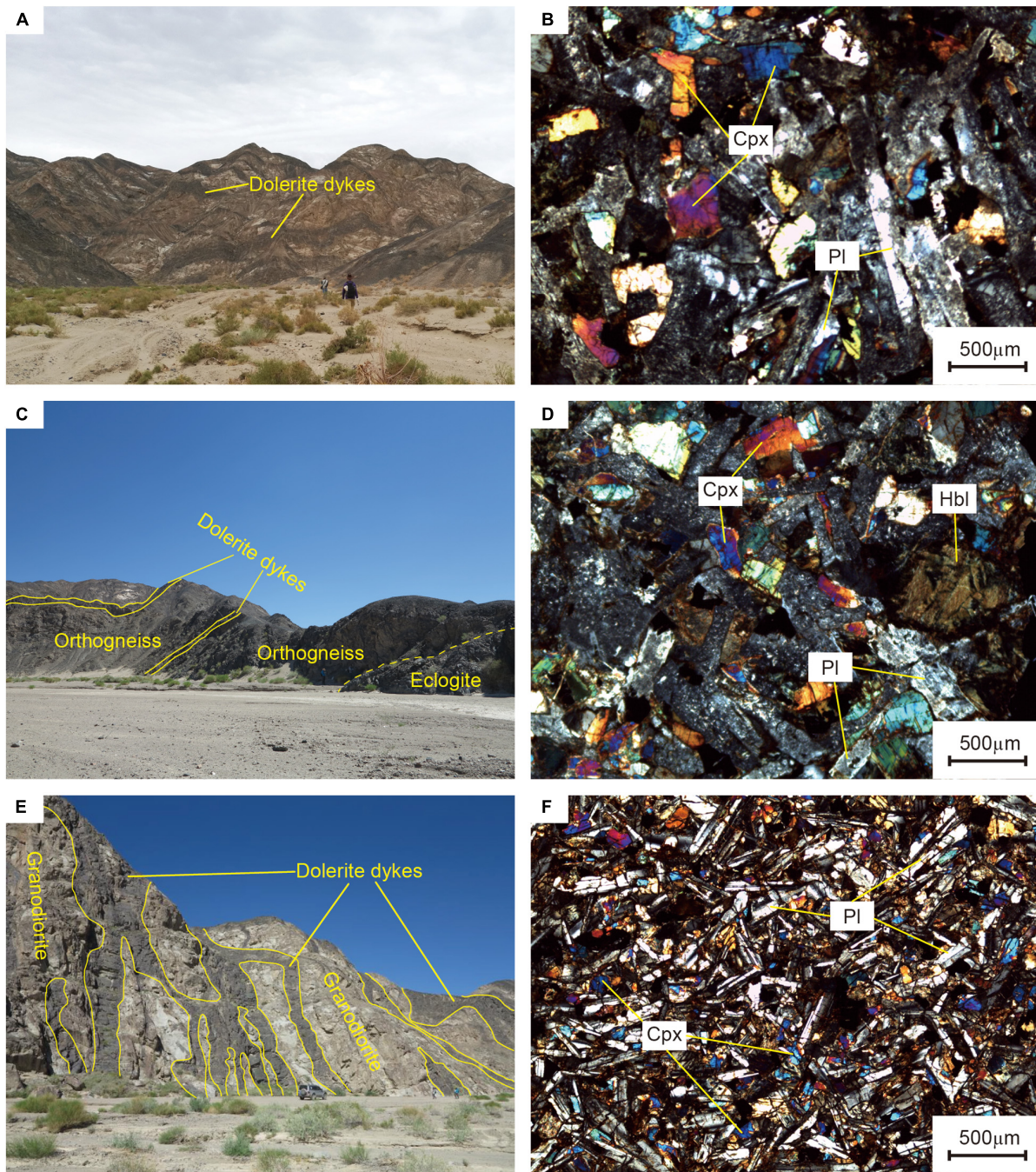


FIGURE 2 | Outcrops of dolerite dykes and photomicrographs of representative dolerite dykes from Gubaoquan. **(A)** Gubaoquan Dolerite dykes intruded into Precambrian orthogneisses. **(C)** Gubaoquan dikes between orthogneisses and eclogite. **(E)** Gubaoquan dikes intruded into Silurian-Devonian granodiorite country rocks. **(B,D)** Clinopyroxene, plagioclase and hornblende within the Gubaoquan dikes. **(F)** Showing the ophitic texture. Cpx, clinopyroxene; Pl, plagioclase; and Hbl, hornblende.

conditions were: 15-kV accelerating voltage, 20-nA beam current, 1- μ m beam size, and a 20-s peak counting time. International mineral standards were used for calibration. Analytical reproducibility was within $\pm 2\%$ relative.

Whole-rock major and trace element compositions were determined at Chang'an University, China. The major element

concentrations were measured by X-ray fluorescence (XRF) spectrometer (Shimadzu 1800) on fused glass disks, and Chinese national rock standards GBW07112 (gabbro) was used for calibration. Analytical precision for major elements was less than 3%. Whole-rock trace elements analyses were performed using a American Thermoelectric X-7 ICP-MS instrument, at

Chang'an University. Sample powder (40mg) were acid-digested with mixed HNO₃ and HF in steel-bomb coated Teflon beakers for 48 h in order to ensure complete dissolution of refractory minerals. Take the USGS basalt standard BCR-2 as external standard sample to calibrate the trace elemental concentrations of the measured samples, and analytical precision was generally better than 5%.

Whole-rock Sr–Nd isotopic analyses were undertaken using a Nu Plasma HR multi-collector (MC) ICP–MS instrument at State Key Laboratory of Continental Dynamics, Northwest University. Detailed descriptions of analytical procedures can be found in Zong (2013). The measured ¹⁴³Nd/¹⁴⁴Nd and ⁸⁷Sr/⁸⁶Sr ratios were normalized to ¹⁴⁶Nd/¹⁴⁴Nd = 0.7219 and ⁸⁶Sr/⁸⁸Sr = 0.1194, respectively. Repeated analysis of the NBS987 and Shin-Etsu JNdi-1 standards yielded ⁸⁷Sr/⁸⁸Sr and ¹⁴³Nd/¹⁴⁴Nd ratios of 0.710248 ± 0.000012 (2σ) and 0.512116 ± 0.000009 (2σ), respectively, and the reference values for these standards are ⁸⁷Sr/⁸⁸Sr_{NBS987} = 0.710241 ± 12 (Thirlwall, 1991), ¹⁴³Nd/¹⁴⁴Nd_{JNdi-1} = 0.512110 (Tanaka, 2000). The analytical precision for Sm/Nd and Rb/Sr ratios were below 1%. The total procedural blanks were < 200 pg for Sr and < 100 pg for Nd.

ANALYTICAL RESULTS

Zircon U–Pb Age

Zircon U–Pb data for the Gubaoquan mafic dykes are listed in Table 1. Sample GBQ-04 was collected from a mafic dyke in the Gubaoquan area that was intruded into Silurian–Devonian granodiorite (424–380 Ma; Mao et al., 2010) and Precambrian orthogneisses (Figures 2A,C; Yang et al., 2006; Mao, 2008; Saktura et al., 2017). The zircons separated from this sample are colorless and transparent in subhedral granular or columnar shapes, with a length of 50–100 μm and a length to width ratio of 1:1–2:1. In cathodoluminescence (CL) images, the zircon grains have flat crystal planes, and the majority of these zircons

have well-developed oscillatory zoning, indicating a magmatic origin (Figure 3a). The majority of the older zircon grains have recrystallized blurred zoning and are stubby and subhedral, whereas the three youngest zircons are elongated grain and have more developed oscillatory zoning (Figure 3a). The fourteen measured zircon ²⁰⁶Pb/²³⁸U age values vary in a wide range (Figure 3b). Four zircons yielded Precambrian ages (2044 to 897 Ma), and seven zircons yielded Silurian ages (441 to 425 Ma). In addition, the three youngest ages yield a weighted average age of 280.7 ± 4 Ma (Figure 3b). Accordingly, we interpret the age of 280.7 ± 4 Ma as the emplacement age of the Bubaoquan doleritic dykes, and all older grains as inherited zircons captured from the wall rocks.

Mineral Chemistry

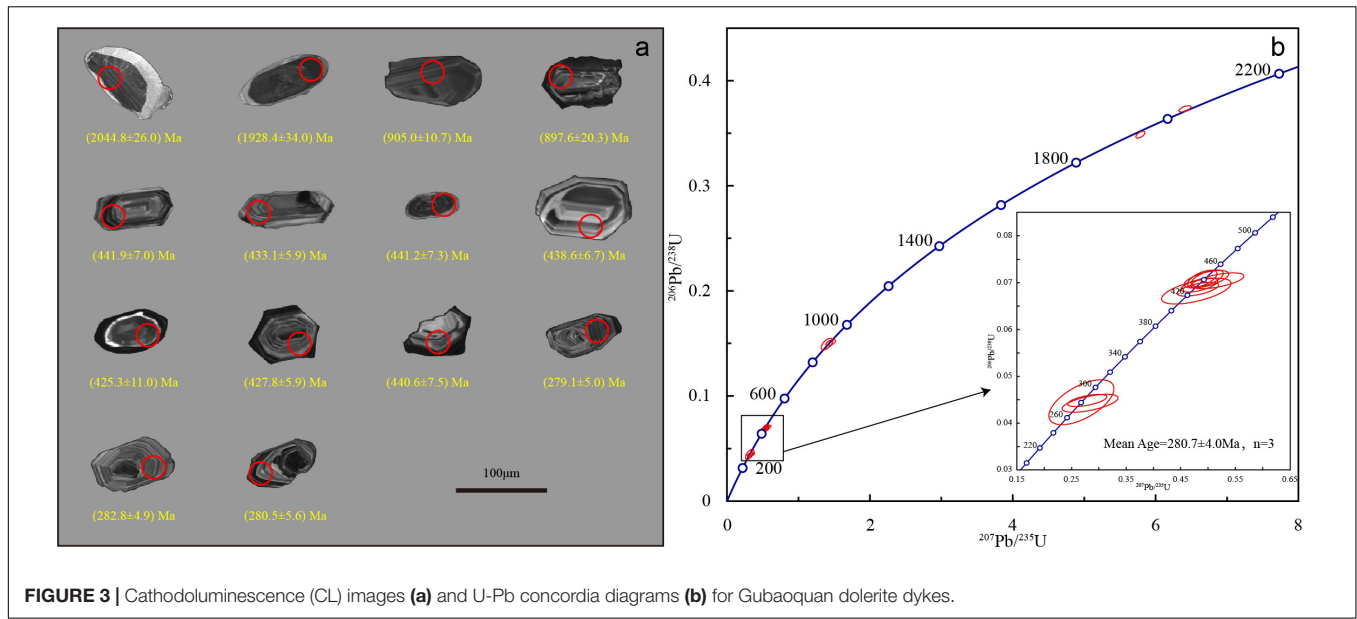
The compositions of clinopyroxene and plagioclase in the Gubaoquan doleritic dykes are given as Supplementary Table 1. Plagioclase within the mafic dykes is mainly labradorite and bytownite with An values of 46.4–74.3 mol%, indicating that plagioclase is the early crystallized mineral from the magma. Clinopyroxene (Wo_{29-6-43.3}En_{30.0-51.2}Fs_{8.8-33.5}) within the doleritic dykes is mainly consist of augite (Wo₃₃₋₄₂En₃₉₋₅₀Fs₁₃₋₂₆), with a small amount of diopside and endiopside (Figure 4). Clinopyroxene from Gubaoquan mafic dykes have the variable Mg# values (47–84), and mainly concentrated in 66 to 84.

Major and Trace Elements

Whole-rock major and trace element compositions of the mafic dykes from the Gubaoquan are given as Supplementary Table 2. The content of whole-rock SiO₂ and Fe₂O₃^T from Gubaoquan dykes ranges from 47.7 to 50.1 wt.% and from 12.5 to 17.4 wt.%, respectively, with relatively lower concentrations of MgO (4.06–5.51 wt.%) and total alkali (Na₂O + K₂O = 2.83–4.37 wt.%). The Mg# values (magnesium index of rock) of the Gubaoquan dolerite are between 41.5 and 57. These dykes are relatively rich

TABLE 1 | Concentrations of U, Th, Pb, and U–Pb isotopes of zircon crystals from a large (25 kg) dolerite sample from the Gubaoquan dolerite dyke.

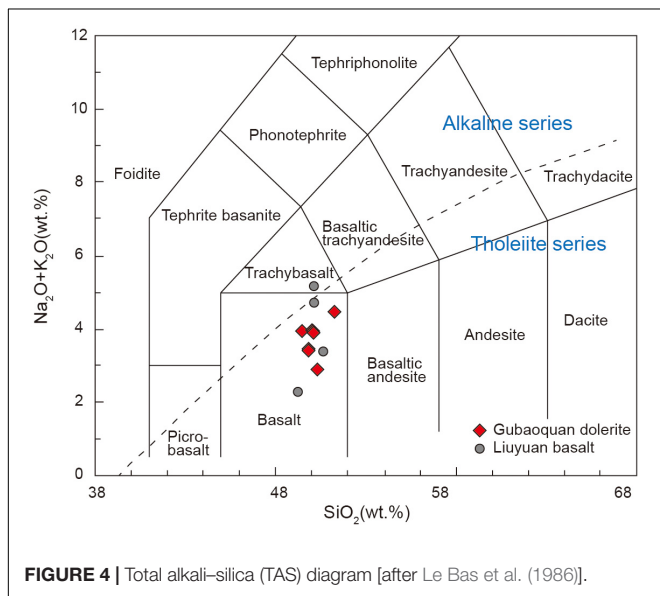
Spot	U	Th	Pb	Th/U	²⁰⁷ Pb/ ²⁰⁶ Pb		²⁰⁷ Pb/ ²³⁵ U		²⁰⁶ Pb/ ²³⁸ U		²⁰⁶ Pb/ ²³⁸ U	
	ppm	ppm	ppm		Ratio	1σ	Ratio	1σ	Ratio	1σ	Age (Ma)	1σ
GBQ-04-01	482	142	38	0.30	0.055607	0.002092	0.534197	0.022213	0.069493	0.000983	433.1	5.9
GBQ-04-02	812	305	69	0.38	0.055787	0.001699	0.548701	0.019399	0.070958	0.001169	441.9	7.0
GBQ-04-03	896	296	69	0.33	0.054952	0.001661	0.539530	0.017815	0.070837	0.001207	441.2	7.3
GBQ-04-04	403	190	38	0.47	0.055594	0.003802	0.528526	0.042042	0.068207	0.001818	425.3	11.0
GBQ-04-05	649	248	55	0.38	0.055658	0.002584	0.531442	0.025080	0.068616	0.000974	427.8	5.9
GBQ-04-06	446	308	112	0.69	0.068421	0.002588	1.399316	0.053892	0.149408	0.003623	897.6	20.3
GBQ-04-07	451	120	68	0.27	0.069355	0.002308	1.451242	0.045158	0.150718	0.001913	905.0	10.7
GBQ-04-08	267	131	28	0.49	0.057753	0.003236	0.567486	0.031822	0.070407	0.001114	438.6	6.7
GBQ-04-09	434	183	39	0.42	0.055745	0.002878	0.547047	0.026929	0.070744	0.001238	440.6	7.5
GBQ-04-12	349	238	13	0.68	0.052223	0.003409	0.333921	0.033872	0.044252	0.001264	279.1	5.0
GBQ-04-14	349	83	13	0.24	0.052673	0.002826	0.328714	0.023732	0.044854	0.000854	280.5	5.6
GBQ-04-15	676	352	26	0.52	0.055816	0.003224	0.318270	0.039358	0.044471	0.003167	282.8	4.9
GBQ-04-17	488	141	156	0.29	0.124542	0.002452	6.409970	0.056531	0.373285	0.001946	2044.8	26.0
GBQ-04-18	1632	125	489	0.08	0.120357	0.002013	5.786799	0.042245	0.348710	0.002171	1928.4	34.0



in iron and poor in magnesium thereby belonging to iron-rich mafic rock group, and are also sub-alkaline and basaltic in a TAS diagram (Figure 5; Le Bas et al., 1986), that is similar to the major element characteristics of dolerites in the Yinwaxia and Podong areas (Zhang et al., 2015; Xue et al., 2016), whereas the type of dolerite formed in the same period in the Tarim Bachu area is dominantly alkaline basalt (Yu, 2009).

The chondrite-normalized rare-earth element (REE) patterns and primitive mantle-normalized immobile incompatible element patterns are illustrated in Figures 6A,B. The Gubaoquan dykes show slightly depleted to enriched LREE patterns ($[La/Yb]_N = 0.93-1.32$) and weakly negative Eu anomalies ($\delta Eu = 0.87-0.99$; Figure 6A), which may be caused by the

distribution of Eu in the magma into the early crystallized plagioclase. The samples from the Gubaoquan doleritic dykes have lower Ni (14.9–62.9 ppm) and Cr (12–132 ppm) concentrations and lower Nb/La (0.33–0.41), Nb/Ta (10.64–14.48), Nb/Y (0.05–0.07) ratios, but higher Th/La (0.12–0.15) and Zr/Nb (48.2–56.2) ratios than the primitive mantle (McDonough and Sun, 1995). As show in Figure 6B, the samples are characterized by pronounced Nb-Ta negative anomalies and slightly light REE enrichments relative to heavy REE, that is similar to the trace element distribution characteristics of the Mesozoic island arc basalts. Compared with the regional contemporaneous dykes and basalt, the Liuyuan basalt is relatively more enriched in LREE and HFSE, while the Gubaoquan dykes have slightly higher trace element content than that of doleritic dykes in the Yinwaxia and Podong areas. However, they have similar distribution patterns of rare earth elements and trace elements which are significantly different from the geochemical characteristics of Bachu mafic dykes of the same period in the Tarim area.



Sr-Nd Isotopes

The Rb-Sr and Sm-Nd contents and isotopic composition of the Gubaoquan dykes are listed in Table 2. The $\epsilon Nd (t = 280 \text{ Ma})$ value of the Gubaoquan dolerites ranges from 6.4 to 6.8, similar to the values of dolerites in Yinwaxia [$\epsilon Nd (t) = 9.0-9.1$; Zhang et al., 2015] and Podong [$\epsilon Nd (t) = 5.5-7.4$; Xue et al., 2016], and shows the characteristics of depleted mantle, which is different from the Bachu dolerite in the Tarim area [$\epsilon Nd (t) = -1.2-3.5$; Jiang et al., 2004b; Yu, 2009; Yu et al., 2017]. The Gubaoquan doleritic dykes have variably and higher initial $^{87}Sr/^{86}Sr$ ratios (0.706240 to 0.707626) than the ratios of dolerites in Yinwaxia (0.703622 to 0.704141; Zhang et al., 2015) and Podong (0.704042 to 0.705267; Xue et al., 2016), which may be attributed to a certain degree of crustal contamination during magma ascent and emplacement. The relatively low initial $^{87}Sr/^{86}Sr$ ratios and

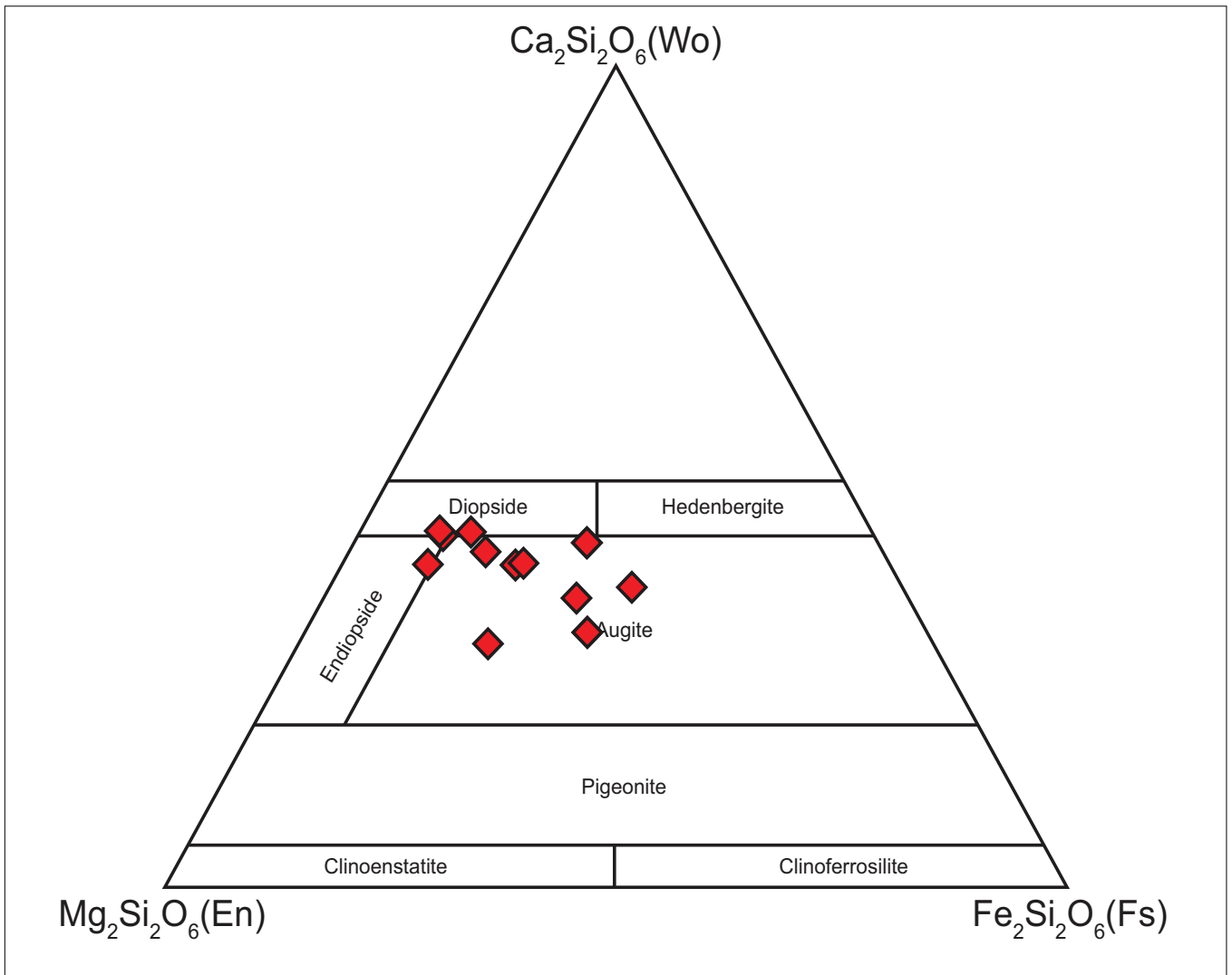


FIGURE 5 | CaSiO_3 (Wo) - MgSiO_3 (En) - FeSiO_3 (Fs) diagram showing the compositions of pyroxene (after Morimoto, 1988) from the Gubaoquan dolerite dykes.

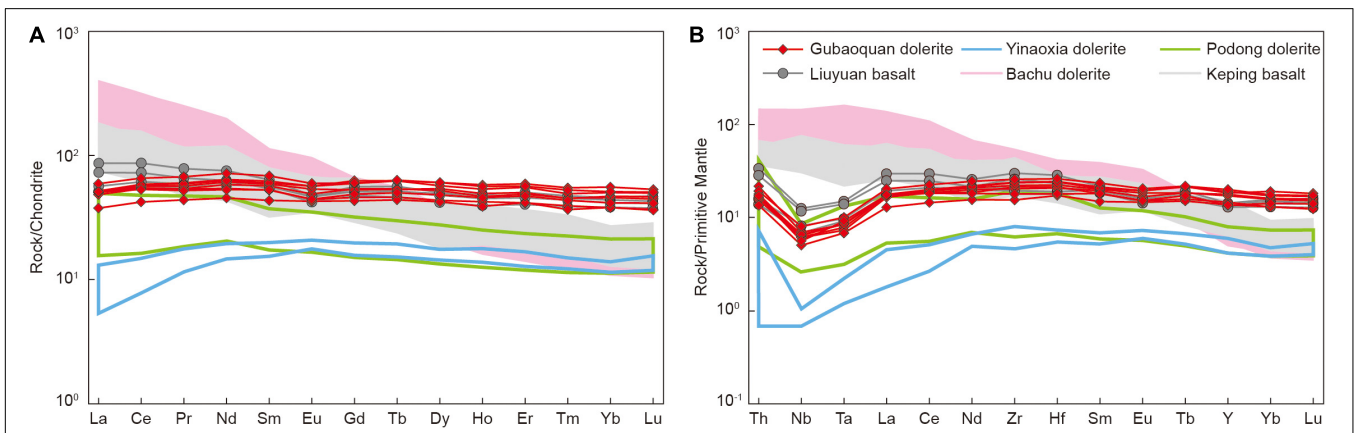


FIGURE 6 | **(A)** Chondrite-normalized REE patterns and **(B)** primitive mantle-normalized immobile element patterns for the Gubaoquan dolerite dykes. Normalizing values from Sun and McDonough (1989). Data sources: Yinaoxia dkes (Zhang et al., 2015), Podong dykes (Xue et al., 2016), Tarim Bachu dolerite dikes (Yu, 2009), and Tarim Keping basalt (Jiang et al., 2004a).

TABLE 2 | Sm-Nd and Rb-Sr isotopic analytical results of the Gubaoquan dolerite dykes in the Beishan area, NW China.

Sample	Rb (ppm)	Sr (ppm)	⁸⁷ Rb/ ⁸⁶ Sr	⁸⁷ Sr/ ⁸⁶ Sr	2σ	(⁸⁷ Sr/ ⁸⁶ Sr) _i	Sm (ppm)	Nd (ppm)	¹⁴⁷ Sm/ ¹⁴⁴ Nd	¹⁴³ Nd/ ¹⁴⁴ Nd	2σ	(¹⁴³ Nd/ ¹⁴⁴ Nd) _i	ε Nd(t)
GBQ-1b	34.8	137	0.7375	0.710174	0.000016	0.707183	9.48	29.8	0.1937	0.512964	1.1E-05	0.512602	6.5
GBQ-5a	38.1	170	0.6466	0.710168	0.000013	0.707546	8.95	28.4	0.1918	0.512971	8E-06	0.512613	6.7
GBQ-6a	43.8	157	0.8076	0.710901	0.000012	0.707626	9.17	29.2	0.1913	0.512975	6E-06	0.512618	6.8
GBQ-7a	29.2	151	0.5612	0.708516	0.000016	0.706240	6.62	21.1	0.1907	0.512966	0.00001	0.512610	6.6
GBQ-9a	36.9	160	0.6678	0.709702	0.000014	0.706994	10.5	33.4	0.1908	0.512954	9E-06	0.512598	6.4

high εNd (t) values (Figure 7) are similar to the mafic dykes in Podong and Yinaoxia. It is also similar to the Liuyuan mafic-ultramafic intrusions and basalts [εNd (t) = -1.84–9.0; initial ⁸⁷Sr/⁸⁶Sr = 0.703390–0.7098] which are thought to have been derived from a depleted asthenospheric mantle source (Zhao et al., 2006; Mao et al., 2012).

DISCUSSION

Age of Doleritic Dykes

Dolerite belongs to a mafic hypabyssal intrusive rock. The primitive magma was silica-unsaturated, and dolerite was formed during the rapid ascent and emplacement of magma. Therefore,

primary magmatic zircons are difficult to crystallize in dolerite. Considering the fact that mafic dykes are able to capture zircons from their wall rocks during ascent, the majority of these zircons can be interpreted as xenocrysts captured from wall rocks.

Previous data show that Precambrian metamorphic basement were extensively developed in Beishan area (China University of Geosciences Press, 1997; Niu et al., 2020). The doleritic dykes from Gubaoquan area mainly intruded the Silurian–Devonian granodiorite (424–380 Ma; Mao et al., 2010) and Precambrian orthogneisses (Figures 2A,C; Yang et al., 2006; Mao, 2008; Saktura et al., 2017), respectively. It is inferred that the formation age of the Gubaoquan doleritic dykes should be later than the Devonian. This means that the three youngest zircons (279.1, 280.5, and 282.8 Ma) are most likely to crystallize from the mafic magma, and their weighted average ²⁰⁶Pb/²³⁸U age of 280.7 ± 4 Ma can be taken as the best estimation of the emplacement age of the Gubaoquan dykes. Whereas, the older age groups (2044–897 Ma and 441–425 Ma) represent the ages of zircons captured from the basement strata (Precambrian orthogneisses) and country rocks (granodiorite) during the ascent of magma. In addition, According to the statistics of the age of doleritic dykes (Table 3) in the Beishan area, the emplacement age range of the dolerite dyke swarms is 271.2 ± 2.9–313.6 ± 3.3 Ma, and concentrated in 285–270 Ma, similar to that of the mafic dykes in Podong, Huaniushan, and Yinwaxia area. Moreover, the age of doleritic dykes obtained by Zhang et al. (2015) in the Liuyuan Gubaoquan area is 282 Ma, indicating that there was extensive mafic magmatism from the Late Carboniferous to Early Permian in the Beishan area.

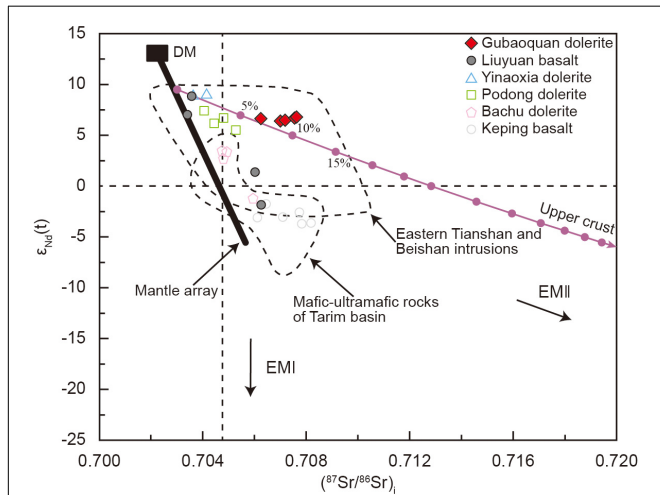


FIGURE 7 | Plot of εNd (t) versus initial ⁸⁷Sr/⁸⁶Sr isotopic ratios for dolerite dykes and basalt in Beishan and Tarim areas. Data for intrusions within the eastern Tianshan and Beishan areas are from Zhou et al. (2004), Qin et al. (2011), Song et al. (2011), and Zhang et al. (2011). Data sources for Permian magmatism of the Tarim LIP are from Jiang et al. (2004a), Yu (2009), Zhou et al. (2009), Xie et al. (2014), and Wei et al. (2014). Data sources: Yinaoxia dykes (Zhang et al., 2015), Podong dykes (Xue et al., 2016), Tarim Bachu dolerite dykes (Yu, 2009), Tarim Keping basalt (Jiang et al., 2004a), and Liuyuan basalt (Zhao et al., 2006). Values used in the mixing calculation: (1) upper crust, 27 ppm Nd, 320 ppm Sr, εNd (t) = -6, (⁸⁷Sr/⁸⁶Sr)_i = 0.72; (2) mantle-derived magma, 7.3 ppm Nd, 90 ppm Sr, εNd (t) = 9.5, (⁸⁷Sr/⁸⁶Sr)_i = 0.703. Concentrations of immobile elements: Depleted mantle is from Sun and McDonough (1989), upper crust is from Rudnick and Gao (2014). The Sr-Nd isotopic array for magmas derived from oceanic mantle is from Zindler and Hart (1986).

Magma Source and Crustal Contamination

The results of the whole-rock Sr-Nd isotopic simulation reveal that the magma of the Gubaoquan doleritic dykes experienced contamination with upper-crust materials during the emplacement. In the simulation, the two-component of the magma isotopic composition are taken from the primitive mantle that is the intersection point between the sample and the mantle trend line [εNd (t) = 9.5, (⁸⁷Sr/⁸⁶Sr)_i = 0.703], and the upper crust [Rudnick and Gao, 2014; εNd (t) = 6, (⁸⁷Sr/⁸⁶Sr)_i = 0.72]. The magma evolved from the depleted mantle has Sr and Nd concentrations of 90 ppm and 7.3 ppm, respectively. The Sr and Nd concentrations of upper-crust contaminant end members are assumed to be 320 ppm and 27 ppm, respectively. These values lie within the mean value ranges of oceanic basalts and upper crust, respectively (Sun and McDonough, 1989; Rudnick

and Gao, 2014). The simulation calculation results show that the Gubaoquan mafic dykes have a crustal contamination degree of 5~10% (Figure 7), which is close to the Liuyuan basalts and higher than the doleritic dykes in Yinwaxia and Pobei areas. In addition, the presence of xenocrystic zircons from the Precambrian strata and granodiorite provided the evidence for crustal contamination during the magma emplacement.

Mafic magma generally originates from the asthenosphere or lithospheric mantle (Fiona et al., 2017). The Fe/Mn ratios of mafic rocks can be used to identify their parental magma composition (Liu et al., 2008). In general, MORB have the lower Fe/Mn ratios (55–58; Zhang et al., 2011) than the plume-derived basalts such as Hawaiian OIBs (about 65–71; Humayun et al., 2004) and continental flood basalts (~ 63.7; Wang et al., 2011). Olivine and clinopyroxene fractionation will decrease and increase Fe/Mn ratios, respectively (Liu et al., 2008). The relatively uniform Fe/Mn ratios (54.1–59.7) of the Gubaoquan doleritic dykes is similar to the MORB, and suggest that the crystallization of olivine and pyroxene has little overall impact on the Fe/Mn ratio of the magma. This reveals that the Fe/Mn ratios of the Gubaoquan dykes reflect the composition of their mantle source and imply a MORB-type parental magma. In addition, the $\epsilon\text{Nd}(t)$ value of the Gubaoquan doleritic dykes varies between 6.4 and 6.8, showing the characteristics of a depleted mantle. All of the mafic dykes plot above the MORB-OIB array on a Th/Yb versus Nb/Yb diagram, that are similar to Liuyuan basalts, Podong and Yinaoxia doleritic dykes (Figure 8), further suggesting the involvement of a subduction-related component (Pearce, 2008). However, the Bachu doleritic dykes and Keping basalts plot close to the OIB in the MORB-OIB array, with obvious different sources. Subduction components mainly include siliceous melts and slab-derived fluids, both can impose distinctive geochemical signatures on mantle sources (Pearce, 2005). Highly mobile elements (e.g., Rb, Ba, Cs, and U) are tend to partition into aqueous fluids, whereas Th and LREE are strongly partitioned into sediment-derived siliceous melts (Plank and Wade, 2005). The high and variable Ba/La (5.93–14.2) and Ba/Nb (15.0–37.3) ratios but low Th/Yb (0.17–0.24) ratios of the Gubaoquan doleritic dykes strongly suggest they were derived from a mantle source that was metasomatized by slab-derived fluids (Woodhead

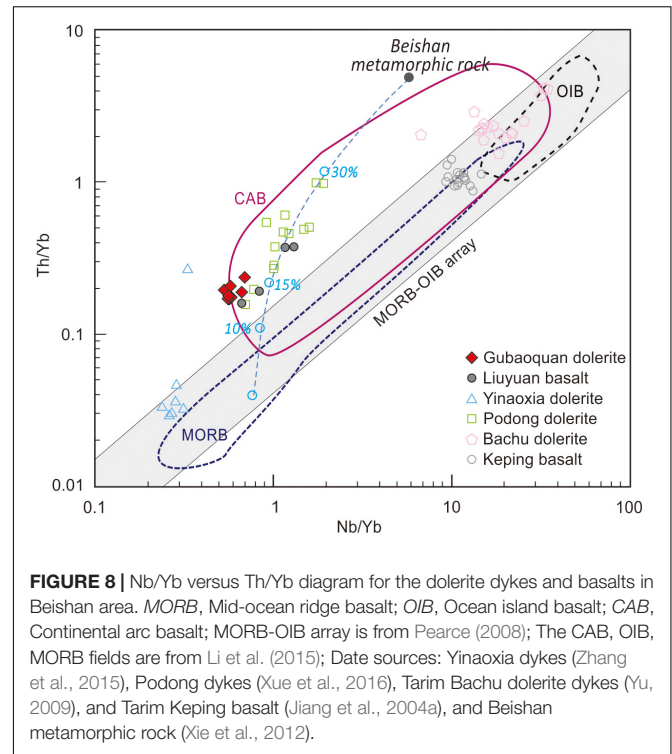


FIGURE 8 | Nb/Yb versus Th/Yb diagram for the dolerite dykes and basalts in Beishan area. MORB, Mid-ocean ridge basalt; OIB, Ocean island basalt; CAB, Continental arc basalt; MORB-OIB array is from Pearce (2008); The CAB, OIB, MORB fields are from Li et al. (2015); Date sources: Yinaoxia dykes (Zhang et al., 2015), Podong dykes (Xue et al., 2016), Tarim Bachu dolerite dykes (Yu, 2009), and Tarim Keping basalt (Jiang et al., 2004a), and Beishan metamorphic rock (Xie et al., 2012).

et al., 2001; Plank and Wade, 2005). Therefore, based on the above results, we propose that the parental magma for the Gubaoquan mafic dykes was derived from the depleted Asthenospheric mantle that metasomatized previously by the subducted fluids, and then contaminated by crustal materials.

Geodynamic Background of Magmatism

The parent magma of these dykes underwent assimilation and contamination with upper-crust materials during the emplacement process, which may have caused of the negative Nb-Ta anomalies in the Gubaoquan dolerite, because the continental crust is severely depleted in Nb and Ta (Rudnick and Gao, 2003). However, there are other possibilities to cause negative Nb-Ta anomalies. Island arc basaltic magma and the mantle-derived magma that was previously metasomatized by a subduction-related component both have the characteristics of negative Nb-Ta anomalies (Rudnick and Gao, 2003; Pearce et al., 2013).

In order to further understand the genesis of negative Nb-Ta anomalies in the Gubaoquan doleritic dykes, we use the whole-rock Nb/Yb and Th/Yb ratios to evaluate the explanations (Pearce, 2008). As shown in Figure 8, the trace element ratios represent the parental magma composition, if we assume that the negative Nb-Ta anomalies in dykes are entirely caused by the contamination with crustal, up to ~15% crustal contamination is required (Figure 8), indicating that the assimilation and contamination with more crustal materials is required to reach the current level of Nb-Ta depletion. As mentioned above, the Sr-Nd isotope compositions of the mafic dykes show significantly lower degrees of crustal contamination (< 10%, Figure 7). The contradiction rules out the possibility of crustal contamination

TABLE 3 | Compiled ages of dolerite dykes in Beishan area.

Location	Rock type	Analytical method	Age (Ma)	Error	Data source
Pobei	Dolerite	SHRIMP	271.2	2.9	Tan (2018)
Podong	Mafic dyke	SIMS	280.5	2.0	Xue et al. (2016)
Cihai	Dolerite	LA-ICP-MS	291.9		Chen et al. (2013)
	Gabbro-dolerite	SIMS	281.9	3.2	Chen et al. (2015)
	Dolerite	SIMS	275.1	2.2	Chen et al. (2015)
Gubaoquan	Dolerite	SIMS	282.0	6.0	Zhang et al. (2015)
Niujuanzi	Mafic dyke	LA-ICP-MS	313.6	3.3	Qi et al. (2017)
Yinaoxia	Dolerite	SIMS	282.0	4.0	Zhang et al. (2015)
		LA-ICP-MS	285.0	4.0	Peng et al. (2020)
Dahongshan	Dolerite	LA-ICP-MS	305.2	2.0	Yang et al. (2015)

as a major cause for the negative Nb-Ta anomalies in the dykes. And the Nb/Yb and Th/Yb ratios of Gubaoquan dykes are within the field of Cenozoic continental arc basalts. The characteristics of trace element and Sr-Nd isotopes indicate that the negative Nb-Ta anomalies probably reflect the primary signature of a mantle source. The parent magma of the Gubaoquan doleritic dykes had a certain degree of Nb-Ta depletion. This shows that the parent magma of the Gubaoquan dykes probably was the basaltic magma in island arc setting or the mantle-derived magma whose source had been metasomatized by subduction fluids before its formation.

The Beishan orogenic belt was formed by the suturing of blocks located in different places in the Paleo-Asian Ocean during the Paleozoic (Zheng et al., 2014, 2016; Chen et al., 2017; Wang et al., 2018). Available geological data have shown that the ophiolite belt in the Beishan area was formed between 330 Ma and 516 Ma (Zhang and Guo, 2008; Li et al., 2012; Zheng et al., 2013; Wang et al., 2014), which represent the upper time limit of the oceanic crust subduction between different blocks. The metamorphic age of the high-temperature and high-pressure metamorphic rock belt distributed across the South Tianshan-Liuyuan-Solonker suture zone on the southernmost margin of CAOB was 465–315 Ma (Gao and Klemd, 2003; Klemd, 2003; Liu et al., 2012; Li et al., 2015; Saktura et al., 2017), which represents the end of oceanic crust subduction, i.e., the subduction of Paleo-Asian oceanic crust ended before the Late Carboniferous (~315 Ma), and subsequently, the stage of arc-continent collision and post-subduction extension was started.

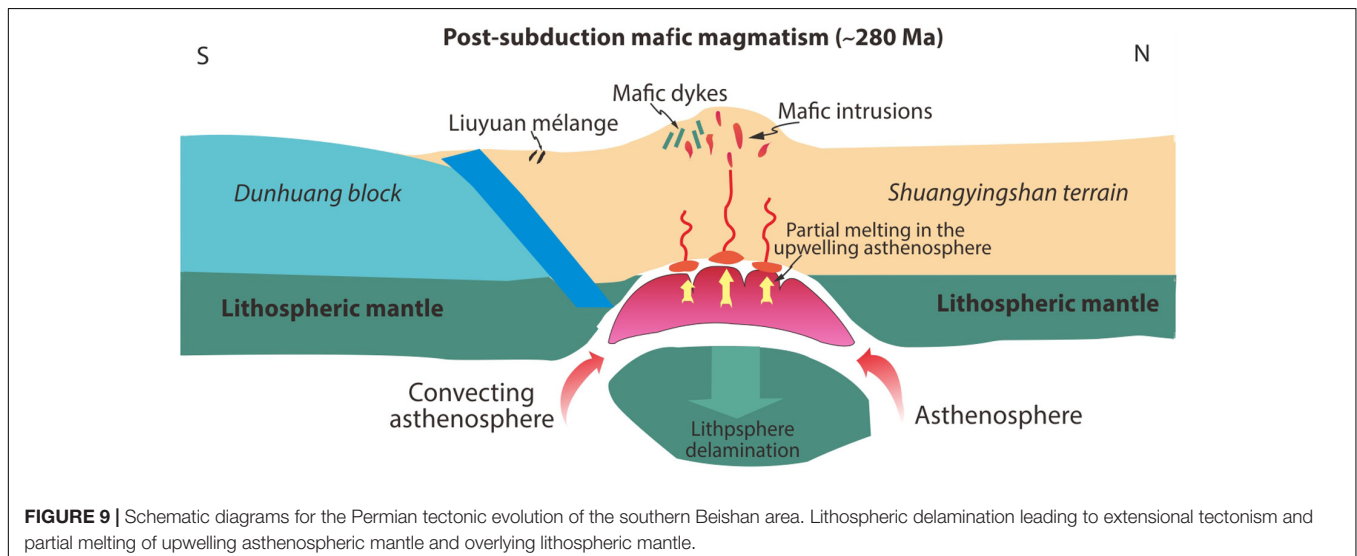
The Gubaoquan dolerite was formed in the Early Permian (~280 Ma). After the subduction of the Paleo-Asian Ocean, the Beishan area has entered the stage of intracontinental evolution. Moreover, considering that there was no arc-related magmatism in the Huaniushan arc or Shibanshan arc since Early Permian. In other words, the significant negative Nb-Ta anomalies in the dykes probably were not formed by the basaltic magma in the island arc setting. Instead, they are the combined results of metasomatism of the mantle-derived magma by fluids from

ancient subducting slab and crustal contamination. The trace rare earth elements and Sr-Nd isotopic characteristics of the Gubaoquan doleritic dykes indicate that its primary magma originated from the depleted asthenosphere mantle, and the magma experienced 5%~10% of assimilation and contamination with upper-crust materials during the emplacement. The petrological and geochemical characteristics of the Gubaoquan doleritic dykes also indicate that they formed under conditions of low water fugacity that are different from the conditions of arc-related basaltic rocks (Feig et al., 2006; Metcalf and Shervais, 2008). Therefore, during the post-subduction extension stage (~280 Ma), lithospheric delamination system was most likely responsible for the genesis of the Permian Gubaoquan mafic dykes in the Beishan area (Figure 9).

Consequently, we suggest that the Gubaoquan doleritic dykes were formed during the tectonic period after the plate subduction. The lithospheric delamination in an extensional environment led to the partial melting of upwelling asthenospheric mantle and the overlying metasomatized mantle, which consequently generated the mafic magma of dolerite. In addition, on a larger scale in Beishan, the formation age of the Gubaoquan doleritic dykes was similar to that of the widely distributed doleritic dykes in the Beishan area, and the Gubaoquan mafic dykes have similar geochemical characteristics to the dykes in the Yinwaxia in the east and Podong in the west. This indicates that the Late Carboniferous to Early Permian doleritic dykes in the Beishan orogenic belt may be controlled by a unified continental geodynamic background, i.e., the dykes are related to the post-subduction extensional setting.

CONCLUSION

Zircon U-Pb dating indicates that the Gubaoquan doleritic dykes in the Beishan orogenic belt were emplaced at ca. 280 Ma, that was the same time as the formation of the dolerite dyke



swarms extensively distribution in Beishan and the Tarim LIP. The geochemical characteristics of these dykes are obviously different from the mafic dykes related to mantle plume activity characterized by OIB-type mantle in Bachu area, Tarim. On the contrary, they are similar to the dykes in Yinaoxia and Podong area. Trace elements and Sr-Nd isotopes indicate that the parental magma for these mafic dykes was derived from the partial melting of the depleted asthenosphere mantle that metasomatized previously by the fluids from ancient subducting slab. This suggests that the dolerite dyke swarms in Beishan area were formed after the closure of the Paleo-Asian Ocean. It was a product of basaltic magmatism formed by the partial melting of the decompressed asthenosphere caused by the lithospheric delamination in a post-subduction extensional setting.

DATA AVAILABILITY STATEMENT

The original contributions presented in the study are included in the article/**Supplementary Material**, further inquiries can be directed to the corresponding authors.

AUTHOR CONTRIBUTIONS

GX: field geological investigation, ideas, formal analysis, and writing – original draft. JD: field geological investigation, validation, and writing – review and editing. WG: data curation and visualization. RW: project administration and validation.

REFERENCES

- Adams, M. G., Lentz, D. R., Shaw, C. S., Williams, P. F., Archibald, D. A., and Cousens, B. (2005). Eocene shoshonitic mafic dykes intruding the Monashee Complex, British Columbia: a petrogenetic relationship with the Kamloops Group volcanic sequence? *Can. J. Earth Sci.* 42, 11–24. doi: 10.1139/e04-091
- Ao, S. J., Xiao, W. J., Han, C. M., Mao, Q. G., and Zhang, J. E. (2010). Geochronology and geochemistry of Early Permian mafic-ultramafic complexes in the Beishan area, Xinjiang, NW China: implications for late Paleozoic tectonic evolution of the southern Altai. *Gondwana Res.* 18, 466–478. doi: 10.1016/j.gr.2010.01.004
- Charvet, J., Shu, L. S., and Laurent-Charvet, S. (2007). Paleozoic structural and geodynamic evolution of eastern Tianshan (NW China): welding of the Tarim and Junggar plates. *Episodes* 30, 162–186.
- Chen, B., Qin, K. Z., Tang, D. M., Mao, Y. J., Feng, H. Y., Xue, S. C., et al. (2015). Lithological, chronological and geochemical characteristics of Cihai iron deposit, Eastern Xinjiang: constraints on genesis of mafic-ultramafic and syenite intrusions and mineralization. *Acta Petrol. Sin.* 31, 2156–2174.
- Chen, C., Xiu, D., Pan, Z. L., Zhang, H., Zhang, J. L., Li, Q. Z., et al. (2017). Early Paleozoic crustal extensional tectonic regime in the central part of Beishan Orogenic Belt: new evidence from geochronology and geochemistry of gabbro in Shibanzhong. *Acta Geol. Sin.* 91, 1661–1673.
- Chen, J. P., Liao, Q. A., Luo, T., Zhang, X. H., Guo, D. B., Zhu, H. L., et al. (2013). Zircon U-Pb geochronology and genesis study on the mafic complex from diabase-type iron deposit in Cihai, Beishan area. *Geol. Sci. Technol. Inform.* 32, 76–83.
- China University of Geosciences Press (1997). *Bureau of Geology and Mineral Resources of Gansu Province*. Zhoukoudian: China University of Geosciences Press.
- Feig, S. T., Jürgen, K., and Snow, J. E. (2006). Effect of water on tholeiitic basalt phase equilibria: an experimental study under oxidizing conditions. *Contrib. Mineral. Petrol.* 152, 611–638. doi: 10.1007/s00410-006-0123-2
- Fiona, C. B., Anthony, J. C., Reid, R. K., and Paul, A. P. (2017). The geology, geochemistry and Ni-Cu-PGE potential of mafic-ultramafic bodies associated with the Dido Batholith, North Queensland, Australia. *Ore Geol. Rev.* 90, 532–552. doi: 10.1016/j.oregeorev.2017.05.002
- Gao, C. L., Ji, R. S., Qin, D. Y., and Yin, Y. (1990). Blueschists in three tectonic environments in northern China. *Geol. Rev.* 36, 20–29.
- Gao, J., and Klemd, R. (2003). Formation of HP-LT rocks and their tectonic implications in the western Tianshan Orogen, NW China: geochemical and age constraints. *Lithos* 66, 1–22. doi: 10.1016/s0024-4937(02)00153-6
- Halls, H. C. (1982). The importance and potential of mafic dyke swarms in studies of geodynamic processes. *Geosci. Canada* 9, 145–154.
- Han, B. F., Guo, Z. J., Zhang, Z. C., Zhang, L., Chen, J. F., and Song, B. (2010). Age, geochemistry, and tectonic implications of a late Paleozoic stitching pluton in the North Tianshan suture zone, western China. *GSA Bull.* 122, 627–640. doi: 10.1130/b26491.1
- Hoek, J. D., and Seitz, H. M. (1995). Continental mafic dyke swarms as tectonic indicators: an example from the Vestfold Hills, East Antarctica. *Precamb. Res.* 75, 121–139. doi: 10.1016/0301-9268(95)80002-y
- Humayun, M., Qin, L. P., and Norman, M. D. (2004). Geochemical evidence for excess iron in the mantle beneath Hawaii. *Science* 306, 91–94. doi: 10.1126/science.1101050
- Jahn, B. M. (2004). The Central Asian Orogenic Belt and growth of the continental crust in the Phanerozoic. *Aspects Tectonic Evol. China* 226, 73–100. doi: 10.1144/gsl.sp.2004.226.01.05
- Jahn, B. M., Wu, F. Y., and Chen, B. (2000). Massive granitoid generation in Central Asia: Nd isotope evidence and implication for continental growth in the Phanerozoic. *Episodes* 23, 82–92. doi: 10.18814/epiugs/2000/v23i2/001

ZS: field geological investigation and visualization. BM: data collection and software. JS: experimental test assistance and software. All authors contributed to the article and approved the submitted version.

FUNDING

This work was financially supported by the National Natural Science Foundation of China (41872076 and 41802081), Shaanxi Natural Science Basic Research Program (2019JQ-674 and 2020JQ-440), and Chang'an University (300102279203).

ACKNOWLEDGMENTS

We are very grateful to Prof. Zhuangzhi Qian, Editor XD, as well as two anonymous reviewers for their encouraging and constructive comments and suggestions in improving this work. Mr. Minwu Liu, Mr. Ke He, and Ms. Chunlei Zong are greatly appreciated for their kind help with geochemical analyses.

SUPPLEMENTARY MATERIAL

The Supplementary Material for this article can be found online at: <https://www.frontiersin.org/articles/10.3389/feart.2021.657716/full#supplementary-material>

- Jiang, C. Y., Zhang, P. B., Lu, D. R., Bai, K. Y., Wang, Y. P., Tang, S. H., et al. (2004a). Petrology, geochemistry and petrogenesis of the Kalpin basalts and their Nd, Sr and Pb isotopic compositions. *Geol. Rev.* 50, 492–500.
- Jiang, C. Y., Zhang, P. B., Lu, D. X., and Bai, K. Y. (2004b). Petrogenesis and magma source of the ultramafic rocks at Wajilitag region, western Tarim Plate in Xinjiang. *Acta Petrol. Sin.* 20, 1433–1444.
- Klemd, R. (2003). Ultrahigh-pressure metamorphism in eclogites from the western Tianshan high-pressure belt (Xinjiang, western China)-comment. *Am. Mineral.* 88, 1153–1156.
- Klemd, R., Gao, J., Li, J. L., and Meyer, M. (2015). Metamorphic evolution of (ultra)-high-pressure subduction-related transient crust in the South Tianshan Orogen (Central Asian Orogenic Belt): geodynamic implications. *Gondwana Res. Int. Geosci. J.* 28, 1–25. doi: 10.1016/j.gr.2014.11.008
- Kröner, A., Windley, B. F., Badarch, G., Tomurtogoo, O., and Martínez, C. (2007). Accretionary growth and crust-formation in the Central Asian Orogenic Belt and comparison with the Arabian-Nubian shield. *Memoir Geol. Soc. Am.* 200, 181–209. doi: 10.1130/2007.1200(11)
- Le Bas, M. J., Le, M. R. W., Streckeisen, A., Zanettin, B., and Rocks, I. S. O. O. I. (1986). A chemical classification of volcanic rocks based on the total alkali-silica diagram. *J. Petrol.* 27, 745–750. doi: 10.1093/petrology/27.3.745
- Li, J. L., Klemd, R., Gao, J., Jiang, T., and Song, Y. H. (2015). A common high-pressure metamorphic evolution of interlayered eclogites and metasediments from the 'ultrahigh-pressure unit' of the Tianshan metamorphic belt in China. *Lithos* 226, 169–182. doi: 10.1016/j.lithos.2014.12.006
- Li, M., Xin, H. T., Ren, B. F., Ren, Y. W., and Liu, W. G. (2020). Early-Middle Permian post-collisional granitoids in the northern Beishan orogen, northwestern China: evidence from U-Pb ages and Sr-Nd-Hf isotopes. *Can. J. Earth Sci.* 57, 681–697. doi: 10.1139/cjes-2019-0088
- Li, S., Wilde, S. A., and Wang, T. (2013). Early Permian post-collisional high-k granitoids from Liuyuan area in southern Beishan orogen, NW China: petrogenesis and tectonic implications. *Lithos* 179, 99–119. doi: 10.1016/j.lithos.2013.08.002
- Li, X. H., Li, W. X., Wang, X. C., Li, Q. L., Liu, Y., and Tang, G. Q. (2009). Role of mantle-derived magma in genesis of early Yanshanian granites in the Nanling Range, South China: in situ zircon Hf-O isotopic constraints. *Sci. China* 52, 1262–1278. doi: 10.1007/s11430-009-0117-9
- Li, X. M., Yu, J. Y., Wang, G. Q., and Wu, P. (2012). Geochronology of Jijitaizi ophiolite in Beishan area, Gansu Province, and its geological significance. *Geol. Bull. China* 31, 2025–2031.
- Liu, L., Wang, C., Cao, Y. T., Chen, D. L., Kang, L., Yang, W. Q., et al. (2012). Geochronology of multi-stage metamorphic events: constraints on episodic zircon growth from the UHP eclogite in the South Altyn, NW China. *Lithos* 136, 10–26. doi: 10.1016/j.lithos.2011.09.014
- Liu, S., Feng, C. X., Jahn, B. M., Hu, R. Z., Gao, S., Coulson, L. M., et al. (2013). Zircon U–Pb age, geochemical, and Sr–Nd–Hf isotopic constraints on the origin of mafic dykes in the Shaanxi Province, North China Craton, China. *Lithos* 175, 244–254. doi: 10.1016/j.lithos.2013.04.020
- Liu, Y. S., Gao, S., Kelemen, B. P., and Xu, W. L. (2008). Recycled crust controls contrasting source compositions of Mesozoic and Cenozoic basalts in the north China craton. *Geochim. Cosmochim. Acta* 72, 2349–2376. doi: 10.1016/j.gca.2008.02.018
- Luan, Y., He, K., and Tan, X. J. (2019). In situ U–Pb dating and trace element determination of standard zircons by LA-ICP-MS. *Geol. Bull. China* 38, 1206–1218.
- Ludwig, K. R. (2003). User's Manual for Isoplot 3.00: a geochronological toolkit for microsoft excel. *Berkeley Geochronol. Center* 125, 197–218.
- Mao, Q. G. (2008). *Paleozoic to Early Mesozoic Accretionary and Collisional Tectonics of the Beishan and Adjacent Area*. Ph. D. Thesis, Chinese Academy of Sciences, Institute of Geology and Geophysics, Beijing.
- Mao, Q. G., Xiao, W. J., Fang, T. H., Wang, J. B., and Han, C. M. (2012). Late Ordovician to early Devonian adakites and Nb-enriched basalts in the Liuyuan area, Beishan, NW China: implications for early Paleozoic slab-melting and crustal growth in the southern Altaid. *Gondwana Res.* 22, 534–553. doi: 10.1016/j.gr.2011.06.006
- Mao, Q. G., Xiao, W. J., Han, C. M., Sun, M., Yuan, C., Zhang, J. E., et al. (2010). Discovery of Middle Silurian adakite granite and its tectonic significance in Liuyuan area, Beishan Moutains, NW China. *Acta Petrol. Sin.* 26, 84–96.
- McDonough, W. F., and Sun, S. S. (1995). The composition of the Earth. *Chem. Geol.* 120, 223–253.
- Metcalfe, R. V., and Shervais, J. W. (2008). Suprasubduction-zone ophiolites: is there really an ophiolite conundrum? *Geol. Soc. Am. Spec. Pap.* 438, 191–222. doi: 10.1130/2008.2438(07)
- Morimoto, N. (1988). Nomenclature of pyroxenes. *Mineral. Petrol.* 39, 55–76. doi: 10.1007/bf01226262
- Niu, Y. Z., Song, B., Zhou, J. L., Xu, W., Shi, J. Z., Zhang, Y. X., et al. (2020). Lithofacies and chronology of volcano-sedimentary sequence in the southern Beishan Region, Central Asian Orogenic Belt and its paleogeographical implication. *Acta Geologica Sinica* 94, 615–633. doi: 10.19762/j.cnki.dizhixuebao.202047
- Pearce, J. A. (2005). *Element Transfer from Slab to Wedge: the Subducted Plate Perspective*. London: AGU Spring Meeting.
- Pearce, J. A. (2008). Geochemical fingerprinting of oceanic basalts with applications to ophiolite classification and the search for Archean oceanic crust. *Lithos* 100, 14–48. doi: 10.1016/j.lithos.2007.06.016
- Pearce, J. A., Stern, R. J., Bloomer, S. H., and Fryer, P. (2013). Geochemical mapping of the Mariana arc-basin system: implications for the nature and distribution of subduction components. *Geochem. Geophys. Geosyst.* 6, 1525–2027.
- Peng, R., Zhang, G. S., and Qiu, H. X. (2020). Petrogenesis and tectonic significances of the late Paleozoic mafic dykes in the Beishan area in Gansu province. *Bull. Mineral. Petrol. Geochem.* 39, 89–101.
- Plank, T., and Wade, J. (2005). *Constraints from Water on Mantle Melting and Slab Fluid Composition*. London: AUG Fall Meeting.
- Qi, Q., Wang, Y. H., Yu, J. Y., Liu, D. M., Guo, L., Ji, B., et al. (2017). Geochronology, geochemistry and tectonic significance of diabase dike swarms in Beishan, Gansu. *Xinjiang Geol.* 35, 99–106.
- Qin, K. Z., Su, B. X., Sakyi, P. A., Tang, D. M., Li, X. H., Sun, H., et al. (2011). SIMS zircon U–Pb geochronology and Sr–Nd isotopes of Ni–Cu-bearing mafic-ultramafic intrusions in eastern Tianshan and Beishan in correlation with flood basalts in Tarim Basin (NW China): constraints on a ca. 280 Ma mantle plume. *Am. J. Sci.* 311, 237–260. doi: 10.2475/03.2011.03
- Rudnick, R. L., and Gao, S. (2003). Composition of the continental crust. *Treatise Geochem.* 3, 1–64. doi: 10.1016/B0-08-043751-6/03016-4
- Rudnick, R., and Gao, S. (2014). Composition of the continental crust. *Treatise Geochem.* 4, 1–51. doi: 10.1016/b0-08-043751-6/03016-4
- Saktura, W. M., Buckman, S., Nutman, A. P., Belousova, E. A., Yan, Z., and Aitchison, J. C. (2017). Continental origin of the Gubaoquan eclogite and implications for evolution of the Beishan Orogen, Central Asian Orogenic Belt, NW China. *Lithos* 294, 20–38. doi: 10.1016/j.lithos.2017.10.004
- Sengör, A. M. C., Natal'in, B. A., and Burtman, V. S. (1993). Evolution of the Altaid tectonic collage and Palaeozoic crustal growth in Eurasia. *Nature* 364, 299–307. doi: 10.1038/364299a0
- Sláma, J., Koler, J., Condon, D. J., Crowley, J. L., Gerdes, A., Hanchar, J. M., et al. (2008). Pleovite zircon—a new natural reference material for U–Pb and Hf isotopic microanalysis. *Chem. Geol.* 71, 1–35. doi: 10.1016/j.chemgeo.2007.11.005
- Song, X. Y., Chen, L. M., Deng, Y. F., and Xie, W. (2013). Syncollisional tholeiitic magmatism induced by asthenosphere upwelling owing to slab detachment at the southern margin of the Central Asian Orogenic Belt. *J. Geol. Soc.* 170, 941–950. doi: 10.1144/jgs2012-130
- Song, X. Y., Xie, W., Deng, Y. F., Crawford, A. J., Zheng, W. Q., Zhou, G. F., et al. (2011). Slab break-off and the formation of Permian mafic-ultramafic intrusions in southern margin of Central Asian Orogenic Belt, Xinjiang, NW China. *Lithos* 127, 128–143. doi: 10.1016/j.lithos.2011.08.011
- Stacey, J. S., and Kramers, J. D. (1975). Approximation of terrestrial lead isotope evolution by a two-stage model. *Earth Planet. Sci. Lett.* 26, 207–221. doi: 10.1016/0012-821x(75)90088-6
- Su, B. X., Qin, K. Z., Sakyi, P. A., Li, X. H., Yang, Y. F., Sun, H., et al. (2011). U–pb ages and Hf–O isotopes of zircons from Late Paleozoic mafic-ultramafic units in the southern Central Asian Orogenic Belt: tectonic implications and evidence for an Early-Permian mantle plume. *Gondwana Res.* 20, 516–531. doi: 10.1016/j.gr.2010.11.015

- Su, B. X., Qin, K. Z., Sakyi, P. A., Tang, D. M., Liu, P. P., Malaviarachchi, S. P. K., et al. (2012). Geochronologic-petrochemical studies of the Hongshishan mafic-ultramafic intrusion, Beishan area, Xinjiang (NW China): petrogenesis and tectonic implications. *Int. Geol. Rev.* 54, 270–289. doi: 10.1080/00206814.2010.543011
- Sun, S. S., and McDonough, W. F. (1989). Chemical and isotopic systematics of oceanic basalts: implications for mantle composition and source processes. *Geol. Soc. Lond. Spec. Publ.* 42, 313–345. doi: 10.1144/gsl.sp.1989.042.01.19
- Tan, L. (2018). *The Study on Magmatic Sequence and Chronology for the Pobei Basic and Ultrabasic Complex in The Northeastern Margin of the Tarim Plate*. Ph. D. Thesis, Chang'an University, Xi'an.
- Tanaka, T. (2000). JNd1: a neodymium isotopic reference in consistency with LaJolla neodymium. *Chem. Geol.* 168, 279–281. doi: 10.1016/s0009-2541(00)00198-4
- Thirlwall, M. F. (1991). Long-term reproducibility of multicollector Sr and Nd isotope ratio analysis. *Chem. Geol.* 94, 85–104. doi: 10.1016/s0009-2541(10)80021-x
- Wang, G. Q., Li, X. M., Xu, X. Y., Yu, J. Y., Ji, B., and Zhu, T. (2018). Petrogenesis and tectonic setting of the Carboniferous and Permian volcanic rocks in the Beishan orogenic belt. *Acta Petrol. Mineral.* 37, 18–34.
- Wang, G. Q., Li, X. M., Xu, X. Y., Yu, J. Y., and Wu, P. (2014). Zircon U-Pb chronological study of the Hongshishan ophiolite in the Beishan area and their tectonic significance. *Acta Petrol. Sin.* 30, 1685–1694.
- Wang, Y., Zhao, Z. F., Zheng, Y. F., and Zhang, J. J. (2011). Geochemical constraints on the nature of mantle source for Cenozoic continental basalts in east-central China. *Lithos* 125, 940–955. doi: 10.1016/j.lithos.2011.05.007
- Wartes, M. A., Carroll, A. R., and Greene, T. J. (2002). Permian sedimentary record of the Turpan-Hami basin and adjacent regions, northwest China: constraints on postamalgamation tectonic evolution. *Geol. Soc. Am. Bull.* 114, 131–152. doi: 10.1130/0016-7606(2002)114<0131:psrott>2.0.co;2
- Wei, X., Xu, Y. G., Feng, Y. X., and Zhao, J. X. (2014). Plume-lithosphere interaction in the generation of the Tarim large igneous province, NW China: geochronological and geochemical constraints. *Am. J. Sci.* 314, 314–356. doi: 10.2475/01.2014.09
- Wiedenbeck, M. (1995). An example of reverse discordance during ion microprobe zircon dating: an artifact of enhanced ion yields from a radiogenic labile Pb. *Chem. Geol.* 125, 197–218. doi: 10.1016/0009-2541(95)00072-t
- Windley, B. F., Alexiev, D., Xiao, W. J., Kröner, A., and Badarch, A. (2007). Tectonic models for accretion of the Central Asian Orogenic Belt. *J. Geol. Soc.* 164, 31–47.
- Woodhead, J. D., Hergt, J. M., Davidson, J. P., and Eggins, S. M. (2001). Hafnium isotope evidence for 'conservative' element mobility during subduction zone processes. *Earth Planet. Sci. Lett.* 192, 331–346. doi: 10.1016/s0012-821x(01)00453-8
- Wu, P., Wang, G. Q., Li, X. M., Yu, J. Y., and Kang, L. (2012). The age of Niujuanzi ophiolite in Beishan area of Gansu Province and its geological significance. *Geol. Bull. China* 31, 2033–2037.
- Xiao, P. X., Huang, Y. H., Wang, Y. X., Wang, X. A., and Li, Y. J. (2006). Geological characteristic and tectonic environment of basic dike swarms in the Beishan area, southern Hami, Xinjiang, China. *Geol. Bull. China* 25, 189–193.
- Xiao, W. J., Han, C. M., Yuan, C., Sun, M., Lin, S. F., Chen, H. L., et al. (2008). Middle Cambrian to Permian subduction-related accretionary orogenesis of Northern Xinjiang, NW China: implications for the tectonic evolution of Central Asia. *J. Asian Earth Sci.* 32, 102–117. doi: 10.1016/j.jseas.2007.10.008
- Xiao, W. J., Huang, B. C., Han, C. M., Sun, S., and Li, J. L. (2011). A review of the western part of the Altai: a key to understanding the architecture of accretionary orogens. *Gondwana Res.* 18, 253–273. doi: 10.1016/j.gr.2010.01.007
- Xiao, W. J., Song, D. F., Han, C. M., Wan, B., Zhang, J., Ao, S. J., et al. (2019). Deep structure and metallogenic processes of the Altai-Junggar-Tianshan collage in southern Altai. *Acta Geol. Sin. Eng. Ed.* 93, 1163–1168. doi: 10.1111/1755-6724.14393
- Xiao, W. J., Zhang, L. C., Qin, K. Z., Sun, S., and Li, J. L. (2004). Paleozoic accretionary and collisional tectonics of the Eastern Tianshan (China): implications for the continental growth of central Asia. *Am. J. Sci.* 304, 370–395. doi: 10.2475/ajs.304.4.370
- Xie, W., Song, X. Y., Deng, Y. F., Wang, Y. S., Ba, D. H., Zheng, W. Q., et al. (2012). Geochemistry and petrogenetic implications of a Late Devonian mafic-ultramafic intrusion at the southern margin of the Central Asian Orogenic Belt. *Lithos* 144, 209–230. doi: 10.1016/j.lithos.2012.03.010
- Xie, W., Xu, Y. G., Feng, Y. X., and Zhao, J. X. (2014). Plume-lithosphere interaction in the generation of the Tarim large igneous province, NW China: geochronological and geochemical constraints. *Am. J. Sci.* 314, 314–356. doi: 10.2475/01.2014.09
- Xue, S. C., Li, C. S., Qin, K. Z., and Tang, D. M. (2016). A non-plume model for the Permian protracted (266–286 Ma) basaltic magmatism in the Beishan-Tianshan region, Xinjiang, Western China. *Lithos* 256, 243–249. doi: 10.1016/j.lithos.2016.04.018
- Xue, S. C., Li, C. S., Wang, Q. F., Ripley, E. M., and Yao, Z. S. (2019). Geochronology, petrology and Sr-Nd-Hf-S isotope geochemistry of the newly-discovered Qixin magmatic Ni-Cu sulfide prospect, southern Central Asian Orogenic Belt, NW China. *Ore Geol. Rev.* 111:103002. doi: 10.1016/j.oregeorev.2019.103002
- Yang, C. X., Wang, Q. H., Gao, X., Pu, W. F., and Zhao, W. (2015). Geochem characteristics and tectonic setting of dolerite in Beishan. *Gansu. Gansu Geol.* 24, 19–23.
- Yang, J. S., Wu, C. L., Chen, S. Y., Shi, R. D., Zhang, J. X., Meng, F. C., et al. (2006). Neoproterozoic eclogitic metamorphic age of the Beishan eclogite of Gansu, China. Evidence from SHRIMP U-Pb isotope dating. *Geol. China* 33, 317–325.
- Yu, J. Y., Li, X. M., Wang, G. Q., Wu, P., and Yan, Q. J. (2012). Zircon U-Pb ages of Huitongshan and Zhangfangshan ophiolite in Beishan of Gansu-Inner Mongolia border area and their significance. *Geol. Bull. China* 32, 2038–2045.
- Yu, X. (2009). *Magma Evolution and Deep Geological Processes of Early Permian Tarim Large Igneous Province*. Ph. D. Thesis, Zhejiang University, Hangzhou.
- Yu, X., Yang, S. F., Chen, H. L., Li, Z. L., and Li, Y. Q. (2017). Petrogenetic model of the permian tarim large igneous province. *Sci. China Earth Sci.* 47, 1179–1190.
- Yuan, F., Zhou, T. F., Zhang, D. Y., Fan, Y., Liu, S., Peng, M. X., et al. (2010). Source, evolution and tectonic setting of the basalts from the native copper mineralization area in eastern Tianshan, Xinjiang. *Acta Petrol. Sin.* 26, 533–546.
- Zhang, Y. Y., Dostal, J., Zhao, Z. H., Liu, C., and Guo, Z. J. (2011). Geochronology, geochemistry and petrogenesis of mafic and ultramafic rocks from Southern Beishan area, NW China: implications for crust-mantle interaction. *Gondwana Res.* 20, 816–830. doi: 10.1016/j.gr.2011.03.008
- Zhang, Y. Y., and Guo, Z. J. (2008). Accurate constraint on formation and emplacement age of Hongliuhe ophiolite, boundary region between Xinjiang and Gansu Provinces and its tectonic implications. *Acta Petrol. Sin.* 24, 803–809.
- Zhang, Y. Y., Yuan, C., Sun, M., Long, X. P., Xia, X. P., Wang, X. Y., et al. (2015). Permian doleritic dikes in the Beishan Orogenic Belt, NW China: asthenosphere-lithosphere interaction in response to slab break-off. *Lithos* 233, 174–192. doi: 10.1016/j.lithos.2015.04.001
- Zhao, Z. H., Guo, Z. J., Han, B. F., Wang, Y., and Liu, C. (2006). Comparative study on Permian basalts from eastern Xinjiang-Beishan area of Gansu province and its tectonic implications. *Acta Petrol. Sin.* 22, 1279–1293.
- Zheng, R. G., Wang, Y. P., Zhang, Z. Y., Zhang, W., Meng, Q. P., and Wu, T. R. (2016). Geochronology and geochemistry of Yinwaxia acidic volcanic rocks in the southern Beishan: new evidence for Permian continental rifting. *Acta Petrol. Mineral.* 37, 18–34.
- Zheng, R. G., Wu, T. R., Zhang, W., Meng, Q. P., and Zhang, Z. Y. (2014). Geochronology and geochemistry of late Paleozoic magmatic rocks in the Yinwaxia area, Beishan: implications for rift magmatism in the southern Central Asian Orogenic Belt. *J. Asian Earth Sci.* 91, 39–55. doi: 10.1016/j.jseas.2014.04.022
- Zheng, R. G., Wu, T. R., Zhang, W., Xu, C., and Meng, Q. P. (2013). Late Paleozoic subduction system in the southern Central Asian Orogenic Belt: evidences from geochronology and geochemistry of the Xiaohuangshan ophiolite in the Beishan orogenic belt. *J. Asian Earth Sci.* 62, 463–475. doi: 10.1016/j.jseas.2012.10.033
- Zheng, R. G., Xiao, W. J., Li, J. Y., Wu, T. R., and Zhang, W. (2018). A Silurian-early Devonian slab window in the southern Central Asian Orogenic Belt: evidence from high-Mg diorites, adakites and granitoids in the western Central Beishan

- region, NW China. *J. Asian Earth Sci.* 153, 75–99. doi: 10.1016/j.jseas.2016.12.008
- Zhou, D. W., Zhang, C. L., Liu, L., Wang, J. L., Wang, Y., and Liu, J. P. (2000). Synthetic study on Proterozoic basic dyke swarms in the Qinling Orogenic Belt and its adjacent block as well as a discussion about some questions related to them. *Acta Petrol. Sin.* 16, 22–28.
- Zhou, M. F., Leshner, C. M., Yang, Z. X., Li, J. W., and Sun, M. (2004). Geochemistry and petrogenesis of 270 Ma Ni-Cu-(PGE) sulfide-bearing mafic intrusions in the Huangshan district, Eastern Xinjiang, Northwest China: implications for the tectonic evolution of the Central Asian Orogenic belt. *Chem. Geol.* 209, 233–257. doi: 10.1016/j.chemgeo.2004.05.005
- Zhou, M. F., Zhao, J. H., Jiang, C. Y., Gao, J. F., Wang, W., and Yang, S. H. (2009). Oib-like, heterogeneous mantle sources of Permian basaltic magmatism in the western Tarim Basin, NW China: implications for a possible Permian large igneous province. *Lithos* 113, 583–594. doi: 10.1016/j.lithos.2009.06.027
- Zindler, A., and Hart, S. R. (1986). Chemical geodynamics. *Annu. Rev. Earth Planet. Sci.* 14, 493–571.
- Zong, C. L. (2013). *Chemical Separation of Pb, Sr, Nd, Hf isotopes from a Single Rock Dissolution and Its Geological Application*. Ph. D. Thesis, Northwest University, Xi'an.

Conflict of Interest: RW was employed by the company Petrochina Changqing Oilfield Company.

The remaining authors declare that the research was conducted in the absence of any commercial or financial relationships that could be construed as a potential conflict of interest.

Copyright © 2021 Xu, Duan, Gao, Wang, Shi, Ma and Sun. This is an open-access article distributed under the terms of the Creative Commons Attribution License (CC BY). The use, distribution or reproduction in other forums is permitted, provided the original author(s) and the copyright owner(s) are credited and that the original publication in this journal is cited, in accordance with accepted academic practice. No use, distribution or reproduction is permitted which does not comply with these terms.